Augmenting a conventional X-ray scanner with edge illumination-based phase contrast imaging: how to design the gratings?

Jonathan Sanctorum[a,b], Nathanaël Six[a,b], Jan Sijbers[a,b], and Jan De Beenhouwer[a,b]

[a]imec-Vision Lab, Department of Physics, University of Antwerp, Belgium
[b]DynXlab: Center for 4D Quantitative X-ray Imaging and Analysis, Antwerp, Belgium

ABSTRACT

Edge illumination is an emerging X-ray phase contrast imaging technique, which has been successfully transferred from synchrotron facilities to lab-based X-ray systems. Rather than installing a dedicated phase contrast system, our goal is to enable phase contrast imaging in a highly flexible X-ray CT system, FleXCT, a novel scanning system consisting of ten motorized axes. These axes allow movements of not only the sample stage, but also the source and detector. To enable phase contrast imaging, two gratings have to be incorporated in the FleXCT system. In this work, we report on the procedure to determine the optimal grating parameters, relying on numerical simulations. Optimal parameter values are presented for both FleXCT gratings.

Keywords: simulation, X-rays, phase contrast, grating, system design, computed tomography

1. INTRODUCTION

Edge illumination (EI) is an emerging X-ray phase contrast imaging (XPCI) technique, which has been successfully transferred from synchrotron facilities to dedicated lab-based X-ray systems.[1,2] XPCI is a valuable tool due to its potential to yield strong image contrast where conventional attenuation-based imaging cannot, e.g. when imaging soft tissue or composite materials.[3] As such, the applications of EI include non-destructive testing,[4] security[5] and (bio)medical imaging.[6] Rather than installing a dedicated XPCI system, our goal is to enable XPCI in a custom-built TESCAN UniTOM XL system (FleXCT) at the University of Antwerp,[7] a novel and highly flexible scanning system consisting of ten motorized axes, allowing a wide range of non-standard scans such as tiled and off-center scans, conveyor belt, laminography, dynamic zooming, and helical tomography. To this end, two gratings have to be incorporated in the existing system, enabling XPCI through the EI technique. The design parameters of these gratings, mainly the pitch, duty cycle and material thickness, determine the achievable image quality. Although other system properties have been shown to influence the image quality as well,[5] these are not necessarily free parameters in our case. As stated, the goal is to augment an existing CT-scanner, for which source and detector are already fixed, as is the maximal system length. Thus, a dedicated parameter study is carried out to determine optimal parameters for the new grating components, relying on numerical XPCI simulations.[8] In this work, we report on the methodology and results of this parameter study.

During the simulation phase, experimental parameters such as the system geometry and focal spot are taken into account. The tube voltage and geometrical magnification are set based on the envisaged applications, one of which will be the imaging of fruit. For the FleXCT system, the goal is to achieve a phase sensitive field of view of approximately 10-by-10 cm^2 in the object plane, with a system magnification of 1.5 and a 80 kV tube voltage. The optimization of the design parameters is based on maximizing peak-to-peak contrast in the phase contrast signal and finding a trade-off between grating bar transmission and shadowing effects (angular filtration).[9] These shadowing effects arise when a cone beam illuminates a pair of flat gratings and are more severe towards the detector edges. Design values for the pitch, aperture and thickness parameters which are considered optimal for the FleXCT system are presented for both gratings. The presented procedure is transferable to other attenuation-based CT-systems and its use is therefore not limited to the FleXCT system. To our best knowledge, this is the first demonstration of grating design for augmentation of an existing X-ray scanner with EI-based XPCI.

Further author information:
J.S.: E-mail: jonathan.sanctorum@uantwerpen.be,
N.S.: E-mail: nathanael.six@uantwerpen.be

2. METHODS

2.1 Edge illumination

EI is a non-interferometric XPCI method, relying on the detection of X-ray refraction in the object.[1,2] This is achieved by introducing two absorbing masks or gratings in the setup, where the first grating is positioned between source and object (sample mask), and the second grating in front of the detector panel (detector mask), as shown in Figure 1. The vertical slits of the sample mask divide the incoming X-ray beam into smaller beamlets. These beamlets subsequently hit the detector mask before reaching the detector. Usually, each beamlet corresponds to a single pixel, and the intensity measured by each pixel is determined by the relative horizontal translation between the two masks. A perfect alignment of the grating slits results in a maximal intensity measurement, whereas fully misaligned masks yield minimal intensity levels. In practice, the varying intensity in every pixel is sampled by horizontally shifting the sample mask relative to the detector mask in a number of discrete steps. This results in the construction of the illumination curve (IC), illustrated in Figure 1, which forms the basis for the retrieval of attenuation, phase, and dark field contrast information from an EI setup.[3] The three signals are calculated from the decrease in surface under the IC, the horizontal shift of the IC, and the IC broadening, respectively.

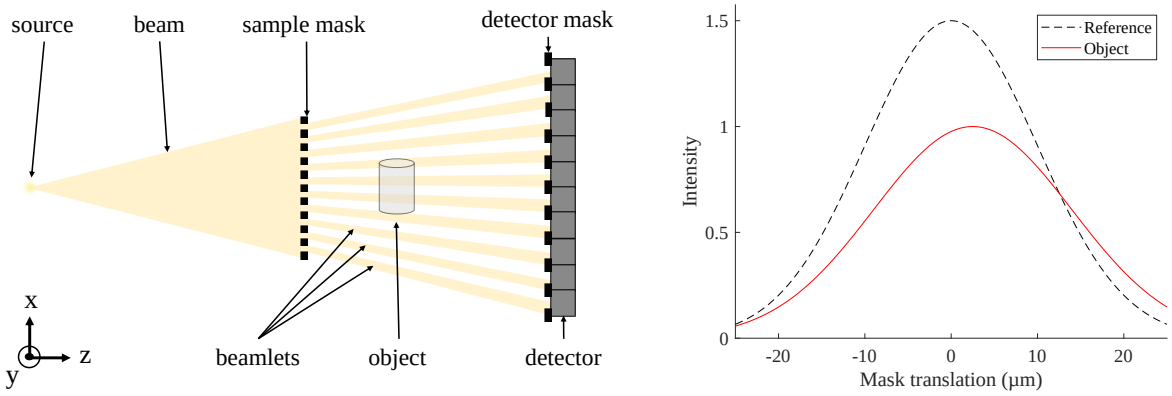

Figure 1. Left: schematic view of an EI setup. Right: IC with and without (reference) object in the beam

2.2 Simulations

Simulations were performed in order to determine the optimal parameters of the gratings required for EI-based XPCI. More specifically, the parameter study is based on Monte Carlo (MC) simulations, for which an in-house modified version of GATE[8,10] is used. Although originally intended for combination with wave optics to perform XPCI simulations of grating-based interferometry, we have demonstrated in earlier work the full-MC simulation of EI experiments using our GATE-based tool.[9,11] In the MC framework, the standard approach is to model grating bars as 3D objects in the simulation, with energy-dependent attenuation properties following from the material. In this work, a virtual grating approach[12] is used to impose grating parameter variations post-simulation, which reduces the total simulation time.

2.3 The FleXCT system

The designed EI gratings are to be incorporated in the FleXCT micro-CT scanner,[7] a customized UniTOM XL model from TESCAN. This highly flexible system allows a wide range of non-standard XCT scans such as tiled and off-center scans, laminography, helical tomography, conveyor belt, and dynamic zooming. Its ten motorized axes enable movement of sample, source, and detector. Additionally, the 'FlexRayTools' software[7] was written to enable the reconstruction of the non-standard XCT projection data using the ASTRA Toolbox, a highly efficient and open source set of tools for tomographic projection and reconstruction.[13] After successful installation of the gratings, the FleXCT system will also facilitate XPCI imaging, including dark field contrast.

3. EXPERIMENTS

Although the FleXCT system has a variable source-to-detector distance (SDD) and geometrical magnification, this choice has to be made prior to optimization of the grating parameters, as the gratings are designed for a specific magnification. Therefore, the SDD remains fixed at 1800 mm in the simulations, with a sample mask magnification of 3/2. Our goal is to achieve an approximately 100 mm by 100 mm sized phase sensitive area in the sample mask plane. The focal spot of the simulated 80 kV polychromatic X-ray source[14] is varied in size and four different spot sizes are considered: 5 μm, 20 μm, 50 μm, and 85 μm. These values correspond to the full width at half maximum (FWHM) of a Gaussian focal spot. Due to the fact that an EI system is only phase sensitive in the direction perpendicular to the grating bars, the simulations are performed using a 1D line detector, for the sake of simulation efficiency. This 1D detector consists of 101 pixels with a pixel size of 150 μm. The detector itself is constructed in GATE from 208 μm thick Gadox, preceded by a 750 μm thick carbon layer and a 250 μm thick plastic layer. In addition, 200 μm amorphous silicon is introduced behind the Gadox layer. A beryllium cylinder with a diameter of $\sim$ 6.9 mm is used as a phantom in the simulations. Sample mask apertures in the range of 5 to 50 μm are considered, whereas for each sample mask aperture three distinct detector mask aperture sizes are simulated, corresponding to 1.5, 1.6, or 1.7 times the sample mask aperture. Seven phase steps are performed to sample the IC, in combination with three dithering steps. In total, this results in 15456 generated profiles, including 3864 flat field profiles. The thickness of the gold grating bars is determined through a trade-off between grating bar transmission and grating bar shadowing (angular filtration), for which separate MC simulations are performed. In these simulations, the bar thickness is varied between 150 μm and 350 μm and different levels of Al filtration are considered.

4. RESULTS AND DISCUSSION

Figure 2 shows the transmission through the grating bar material for an increasing gold layer thickness and different effective spectra, resulting from filtration by 0.5 mm, 1.0 mm and 2.0 mm of aluminum. Ideally, the transmission should be below 1%, although 5% is an acceptable level of transmission for EI systems.[5] The plot indicates that, for the envisaged tube voltage of 80 kV, a gold bar thickness greater than 200 μm is required to satisfy this condition. By increasing the thickness further to 350 μm, the ideal 1% transmission level comes within reach.

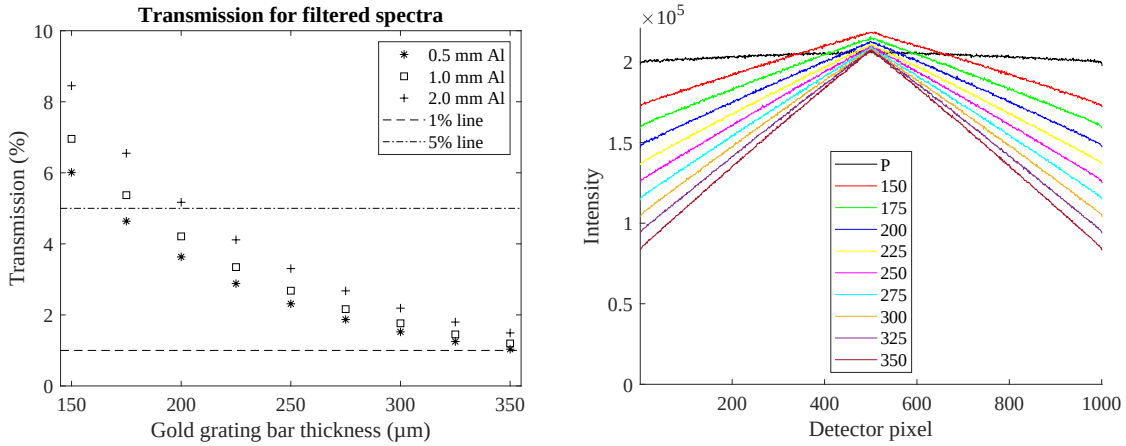

Figure 2. Left: grating bar transmission levels. Right: line profiles for different grating bar thicknesses, legend expressed in μm. The profile resulting from a perfectly absorbing and perfectly flat grating is indicated by P.

Such a large grating thickness, however, introduces a significant amount of shadowing towards the detector edges, as is clear from the line profiles in Figure 2. In this figure, detector line profiles are shown for increasing grating bar thicknesses. As a reference, an additional line profile (P) is plotted, resulting from idealized gratings, which are infinitesimally thin and perfectly absorbing. From comparison to this reference profile, it is clear

that thinner gratings, although resulting in less shadowing, allow more transmission through the grating bars. Hence, there is a trade-off between transmission and shadowing effects. To quantify the amount of shadowing introduced by the grating bars, the ratio between the intensity at the profile edge and the intensity in the center (no shadowing) is determined and plotted in Figure 3. In order to limit shadowing as much as possible while keeping transmission well below the critical 5% level, the optimal thickness of the gold bars is estimated to be 225 μm. This corresponds to an intensity ratio of 65.7%.

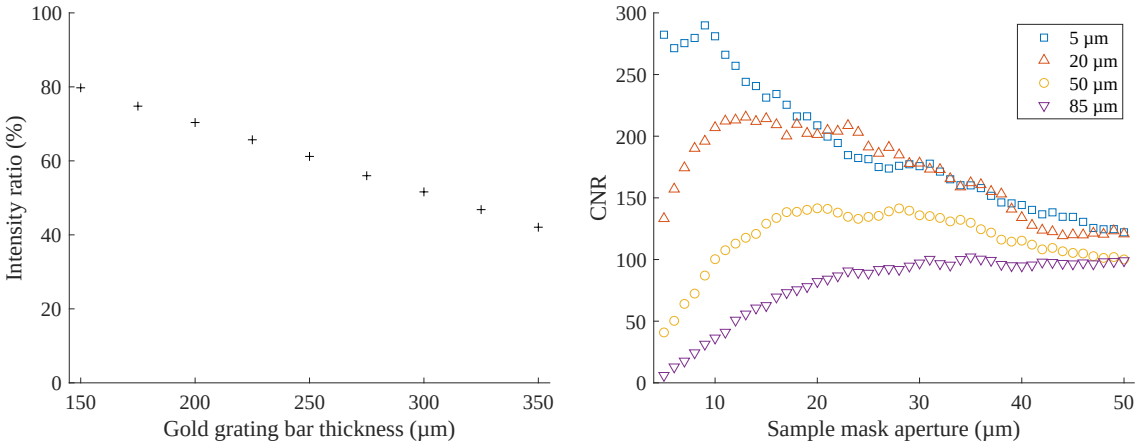

Figure 3. Left: intensity ratio between edge and center pixels. Right: peak-to-peak CNR extracted from the retrieved phase for different focal spot sizes.

As the grating pitches are defined by the SDD and geometrical magnification, the only parameters left to determine are the duty cycles, i.e. the aperture sizes. Given the SDD of 1800 mm, pixel size of 150 μm, and magnification of 1.5, the sample mask pitch must be 100 μm. As the detector mask cannot be put at the exact same position as the detector panel, the pitch should be slightly less than the pixel size: 148 μm. To perform the aperture size optimization, the differential phase in each pixel is retrieved through Gaussian fitting of the sampled IC points. Subsequently, the peak-to-peak contrast is extracted from the resulting profiles and compared to the background fluctuations to yield the contrast-to-noise ratio (CNR). In practice, the peak-to-peak contrast is given by the difference between the positive and negative peak values in the signal. By dividing this by the standard deviation of the background signal, we get the CNR value. The results of this operation are shown in Figure 3 for sample mask aperture values in the range of 5 to 50 μm and a detector mask to sample mask aperture ratio of 1.5. It should be noted that the same amount of photons was simulated for every focal spot. In practice, however, the focal spot size determines the flux: larger focal spots tend to yield a higher flux. By simulating the same amount of photons, we effectively remove this effect from the plot in Figure 3.

The optimal CNR value is reached at different aperture sizes, depending on the focal spot. In practice, some focal spot sizes are more relevant than others. The 5 μm focal spot is close to the smallest focal spot size achievable with the FleXCT system. In EI, however, the majority of the X-rays will be blocked by the gratings. Therefore, the flux generated at the source has to be sufficiently large in order to keep acquisition times reasonable. As such, it is unlikely that the 5 μm spot will be realistic in practice. A spot size around 50 μm, however, is expected to be much more suitable. When the flux has to be maximized, this can be increased to 85 μm, or reduced to 20 μm if less focal spot blur is required. In line with these practical considerations, the optimal sample mask aperture is deduced from the 50 μm focal spot curve in Figure 3, where the maximal CNR is reached around 20 μm. As this value is also virtually optimal for the 20 μm spot and still yields 80% of the maximum CNR for the 85 μm focal spot, a 20 μm aperture is considered to be the best candidate for the optimal sample mask design. No significant CNR gain could be perceived by increasing the aperture size ratio to 1.6 and 1.7, and this ratio was ultimately kept at 1.5. This corresponds to a 30 μm aperture size for the detector mask.

5. CONCLUSION

In this work, we have demonstrated the design of EI gratings for the augmentation of the FleXCT system to a phase sensitive X-ray scanner. Through peak-to-peak contrast analysis of simulated profiles, optimal aperture sizes for sample and detector mask were deduced. In the final grating design, the sample mask has a pitch of 100 μm and aperture of 20 μm, whereas the detector mask has a pitch and aperture size of 148 μm and 30 μm, respectively. Additionally, the material thickness was determined based on a trade-off between shadowing effects and grating bar transmission. Based on this analysis, the gold bar thickness was set to 225 μm. The next important step is the integration and alignment of the newly designed components into the FleXCT system, on which we intend to report in future work. The steps undertaken in this work are not specific to the FleXCT system, and are applicable to support the augmentation of any X-ray scanner with EI-based XPCI.

ACKNOWLEDGMENTS

J. Sanctorum and N. Six contributed equally to the research presented in this work. N. Six has a PhD fellowship of the FWO (11D8319N). This research was also supported by EU Interreg Flanders - Netherlands Smart*Light (0386), Research Foundation - Flanders (FWO) (G090020N, G094320N, S003421N), and Agentschap Innoveren & Ondernemen (Vlaio) (HBC.2020.2159). The authors wish to thank A. Olivo from UCL (UK) for valuable feedback on the simulation results.

REFERENCES

[1] Zamir, A., Hagen, C., Diemoz, P. C., Endrizzi, M., Vittoria, F., Chen, Y., Anastasio, M. A., and Olivo, A., "Recent advances in edge illumination x-ray phase-contrast tomography," *Journal of Medical Imaging* **4**, 040901 (oct 2017).

[2] Olivo, A., "Edge-illumination x-ray phase-contrast imaging," *Journal of Physics: Condensed Matter* **33**, 363002 (sep 2021).

[3] Endrizzi, M., "X-ray phase-contrast imaging," *Nuclear Instruments and Methods in Physics Research A* **878**, 88–98 (JAN 2018).

[4] Shoukroun, D., Massimi, L., Endrizzi, M., Bate, D., Fromme, P., and Olivo, A., "Edge illumination X-ray phase contrast imaging for impact damage detection in CFRP," *Materials Today Communications* **31**, 103279 (jun 2022).

[5] Olivo, A., Ignatyev, K., Munro, P., and Speller, R., "Design and realization of a coded-aperture based X-ray phase contrast imaging for homeland security applications," *Nuclear Instruments and Methods in Physics Research A* **610**, 604–614 (nov 2009).

[6] Massimi, L., Suaris, T., Hagen, C. K., Endrizzi, M., Munro, P. R. T., Havariyoun, G., Hawker, P. M. S., Smit, B., Astolfo, A., Larkin, O. J., Waltham, R. M., Shah, Z., Duffy, S. W., Nelan, R. L., Peel, A., Jones, J. L., Haig, I. G., Bate, D., and Olivo, A., "Volumetric High-Resolution X-Ray Phase-Contrast Virtual Histology of Breast Specimens With a Compact Laboratory System," *IEEE Transactions on Medical Imaging* **41**, 1188–1195 (may 2022).

[7] De Samber, B., Renders, J., Elberfeld, T., Maris, Y., Sanctorum, J., Six, N., Liang, Z., De Beenhouwer, J., and Sijbers, J., "FleXCT: a flexible X-ray CT scanner with 10 degrees of freedom," *Optics Express* **29**, 3438–3457 (feb 2021).

[8] Sanctorum, J., De Beenhouwer, J., and Sijbers, J., "X-ray phase contrast simulation for grating-based interferometry using GATE," *Optics Express* **28**, 33390–33412 (oct 2020).

[9] Huyge, B., Sanctorum, J., Six, N., De Beenhouwer, J., and Sijbers, J., "Analysis Of Flat Fields In Edge Illumination Phase Contrast Imaging," in [*2021 IEEE 18th International Symposium on Biomedical Imaging (ISBI)*], **2021-April**, 1310–1313, IEEE (apr 2021).

[10] Jan, S., Benoit, D., Becheva, E., Carlier, T., Cassol, F., Descourt, P., Frisson, T., Grevillot, L., Guigues, L., Maigne, L., Morel, C., Perrot, Y., Rehfeld, N., Sarrut, D., Schaart, D., Stute, S., Pietrzyk, U., Visvikis, D., Zahra, N., and Buvat, I., "GATE V6: A major enhancement of the GATE simulation platform enabling modelling of CT and radiotherapy," *Physics in Medicine and Biology* **56**(4), 881–901 (2011).

[11] Sanctorum, J., Sijbers, J., and De Beenhouwer, J., "Dark Field Sensitivity In Single Mask Edge Illumination Lung Imaging," in [*2021 IEEE 18th International Symposium on Biomedical Imaging (ISBI)*], **2021-April**, 775–778, IEEE (apr 2021).

[12] Sanctorum, J., Sijbers, J., and De Beenhouwer, J., "Virtual grating approach for Monte Carlo simulations of edge illumination-based x-ray phase contrast imaging." arXiv:2208.04137 [physics.med-ph] (2022).

[13] van Aarle, W., Palenstijn, W. J., Cant, J., Janssens, E., Bleichrodt, F., Dabravolski, A., De Beenhouwer, J., Batenburg, K. J., and Sijbers, J., "Fast and flexible X-ray tomography using the ASTRA toolbox," *Optics Express* **24**(22), 25129–25147 (2016).

[14] Nazemi, E., Six, N., Iuso, D., De Samber, B., Sijbers, J., and De Beenhouwer, J., "Monte-Carlo-Based Estimation of the X-ray Energy Spectrum for CT Artifact Reduction," *Applied Sciences* **11**(7), 3145 (2021).